and for ribosomal protein L27 (RPL27, 5′-CCTCATGCCCACAAGGTACTC-3′ and 3′-TCGCTCCTCAAACTTGACC-5′) as an internal standard.

Total RNA was incubated with DNase I for 30 min and reverse transcription was performed with ReverTra Ace qPCR RT Kit (Toyobo). The relative amount of modulatory calcineurin interacting protein 1 (MCIP1) cDNA was quantified using in the same way as quantification of mtDNA copy number, using the PCR mixture contained 5 ng of the total cDNA, 12 pmol each of primers (5′-TTGGGAACTGTTGGTTGACA-3′ and 5′-ATGGCTACGGCATACTCCAC-3′ for MCIP1) in 30 μl.

In in vivo experiments, 8- to 10-week-old male TFAM overexpression mice and their littermates were used. Under anaesthesia with pentobarbital sodium (30 mg/g BW, i.p.), the hearts were excised and RNA was extracted with RNeasy tissue kit. After reverse transcription, the relative amount of cDNA was quantified using the PCR mixture contained 5 ng of the total cDNA, 12 pmol each of primers (5′-CCGTGTGGAATTGTCCTTCTC-3′ and 5′-GACCCCATGTGCAGAGAAAAC-3′ for MCIP1) in 30 μl. We used hypoxanthine guanine phosphoribosyl transferase (HPRT) gene as an internal standard (5′-CTGGTGAAAAG GACCTCTCG-3′ and 5′-AACTTGCGCTCATCTTAGGC-3′).

2.9. Nuclear translocation of NFAT

In order to assess nuclear translocation of NFAT, production and infection of recombinant adenovirus including green fluorescent protein (GFP)-fused N-terminal region of NFAT4 (we referred as just NFAT in this article) were performed as described previously (Fujii et al., 2005; Nishida et al., 2007). Cardiac myocytes were infected with the adenovirus at a multiplicity of infection of 300 for 60 h. After the stimulation for 30 min with angiotensin II (AngII, 100 nM, Sigma-Aldrich) or ET-1 (100 nM), cells were fixed by 10% formaldehyde (Sigma-Aldrich). The localization of GFP-NFAT was observed at an excitation wavelength of 488 nm with fluorescent microscopy (IX71, Olympus). More than 20 scenes were randomly scanned in each experiment and quantified the subcellular localization of GFP-NFAT using Photoshop (adobe systems).

2.10. Luciferase assays

NFAT-dependent luciferase activity and brain natriuretic peptide (BNP) promoter activity were measured as described previously (Fujii et al., 2005; Nishida et al., 2007, 2010). Cardiac myocytes were transiently co-transfected with 0.45 μg of pNFATLuc (Stratagene) and 0.05 μg of pRL-SV40 (Stratagene) control plasmid or with 0.3 μg of pBNP-Luc and 0.2 μg of pRL-SV40 using Fugene 6 (Roche Diagnostics) for 48 h followed by stimulation of AngII (100 nM) or ET-1 (100 nM). Luciferase activity was measured 6 h (for NFAT) or 24 h (for BNP) after the stimulation using dual luciferase reporter assay system (Promega) according to the manufacturer's protocol.

2.11. Measurement of mitochondrial [Ca^{2+}]

Mitochondrial [Ca^{2+}] was visualized using mitochondria-specific Ca^{2+} indicator, rhod-2/AM (Dojindo). Cardiac myocytes were loaded with 1 μM rhod-2/AM at 37 °C for 30 min. Then they were stimulated with AngII (100 nM) or ET-1 (100 nM), and the time course of fluorescence intensity was traced with a video image analysis system (Aquacosmos, Hamamatsu Photonics).

2.12. Measurement of hypertrophic response of cardiac myocytes

Hypertrophy of cells was assessed by a measurement of cell surface area and amount of actin filament, visualized by actin filament

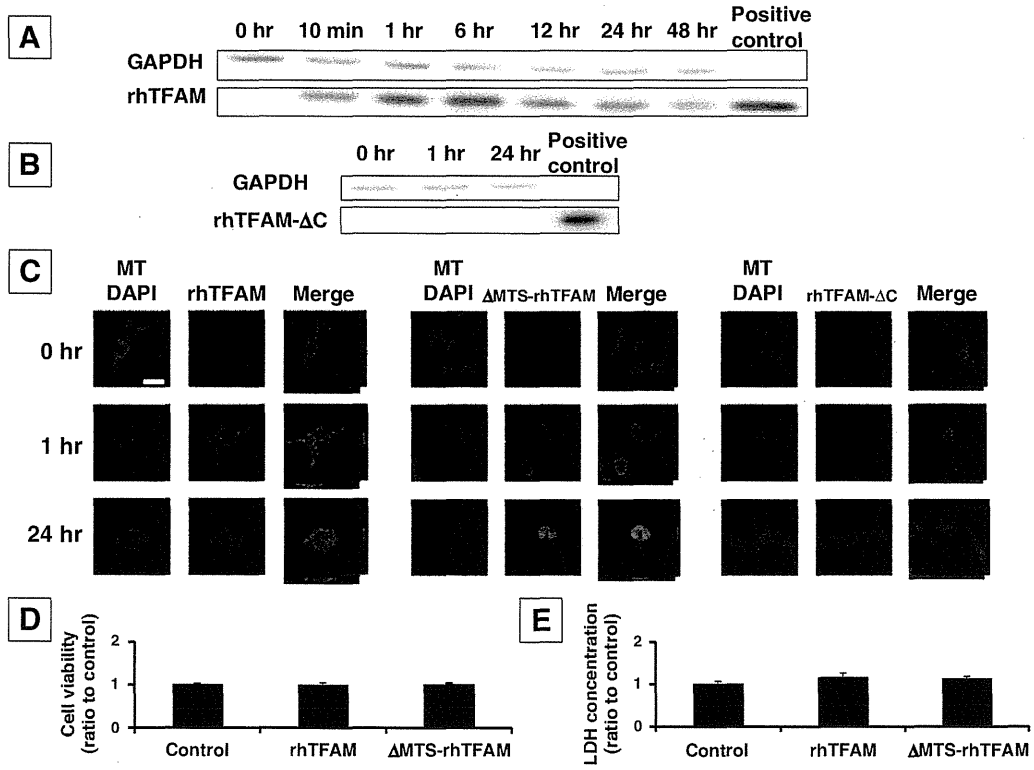

Fig. 2. The localization and cytotoxicity of rhTFAM proteins in cardiac myocytes. (A) Western blot analysis of myocytes treated with rhTFAM protein for 0–48 h. (B) Western blot analysis of myocytes treated with rhTFAM-ΔC protein for 0–24 h. (C) Confocal microscopic observations of myocytes treated with rhTFAM, ΔMTS-rhTFAM, or rhTFAM-ΔC. Red represents mitochondria (MT), green represents human TFAM (Alexa Fluor 488), and blue represents nucleus (DAPI). Scale bar = 20 μm. (D and E) The treatment with rhTFAM or ΔMTS-rhTFAM did not affect the cell viability (D) of myocytes and LDH concentration of the medium (E). Data are presented as ratio to control.

staining. Quantification of hypertrophy of myocytes was performed as previously described (Nishida et al., 2007, 2010). After AngII (100 nM) or ET-1 (100 nM) stimulation for 48 h, cells were fixed by 4% paraformaldehyde (nacalai tesque) and stained with Alexa Fluor 546 phalloidin (Invitrogen) for actin filaments visualization. Digital photographs were taken with confocal microscopy (FV-10i, Olympus) or Biozero Microscope (BZ-8000, Keyence), and the average values of the cell surface area and fluorescent intensity (more than 200 cells) were calculated using BZ-II Analyzer (Keyence).

2.13. Statistical analysis

Data are presented as mean ± standard error. Each experiment was repeated at least three times. Data were analyzed by a two-tailed Student's *t* test or analysis of variance followed by the Tukey post-hoc test with significance imparted at *P* values of <0.05.

3. Results

3.1. rhTFAM was recruited into the mitochondria of cardiac myocytes

We synthesized rhTFAM protein and investigated its recruitment into cardiac myocytes since we expected it as a new therapeutic modality. rhTFAM (100 nM) was just added to the culture medium of myocytes. rhTFAM protein rapidly entered into cultured rat neonatal ventricular myocytes within 10 min of the treatment, and remained in the cells even at 48 h (Fig. 2A). In contrast, rhTFAM-ΔC rarely entered into the cells (Fig. 2B). Confocal microscopy with z-scale analysis revealed that exogenously added rhTFAM localized both in the cytoplasm and mitochondria, whereas ΔMTS-rhTFAM was recruited mostly into the nucleus (Fig. 2C), both for 1 and 24 h treatment. These results suggested that MTS played an important role in determining the localization of recombinant TFAM in myocytes. We confirmed that rhTFAM-ΔC was not recruited into the cells (Fig. 2C), suggesting that some sequence in C-terminal tail of TFAM was important for the recruitment of this protein.

Moreover, ΔMTS-rhTFAM and rhTFAM had no significant cytotoxicity in cardiac myocytes at least at the concentration which we used in these experiments (100 nM), since cell viability did not alter (Fig. 2D) and LDH concentration in culture medium did not increase (Fig. 2E) after the treatment with ΔMTS-rhTFAM or rhTFAM.

3.2. rhTFAM increased mtDNA copy number and mtDNA-encoded proteins

In order to determine whether this recombinant protein functions in cardiac myocytes, we performed characterization of mitochondria after the treatment with rhTFAM. rhTFAM treatment increased mtDNA copy number dose-dependently (0–100 nM) with a maximum increase of approximately two-fold at 12 h, whereas mtDNA copy number was not affected by the treatment with ΔMTS-rhTFAM (Fig. 3A). We confirmed these results by two different PCR primer sets for mtDNA quantification and concluded that rhTFAM recruited into mitochondria functioned and directly increased mtDNA copy number. Using extract from empty vector, we ruled out the possibility that products other than rhTFAM from competent cells increased mtDNA contents (Fig. 3B). The treatment with rhTFAM or ΔMTS-rhTFAM (100 nM) for 24 h did not affect the morphology and the number of mitochondria significantly in cardiac myocytes (Fig. 3C).

To rule out the possibility that the recruitment and function of rhTFAM are the specific property of cardiac myocytes, we used another type of cell, RAW 264.7, to examine whether it also allows rhTFAM to enter into the cells. We found both rhTFAM and ΔMTS-rhTFAM were successfully recruited into RAW 264.7 cells (Fig. 4A and B). Subsequently, rhTFAM functioned to increase mtDNA copy number, but ΔMTS-rhTFAM did not (Fig. 4C). The recruitment and function of rhTFAM were similar to cardiac myocytes, suggesting that they were not unique properties of myocytes, but those of this specific protein.

In order to characterize the change of mitochondrial features by rhTFAM, we investigated the expression of mitochondrial electron transport complex proteins in cardiac myocytes. rhTFAM (100 nM)

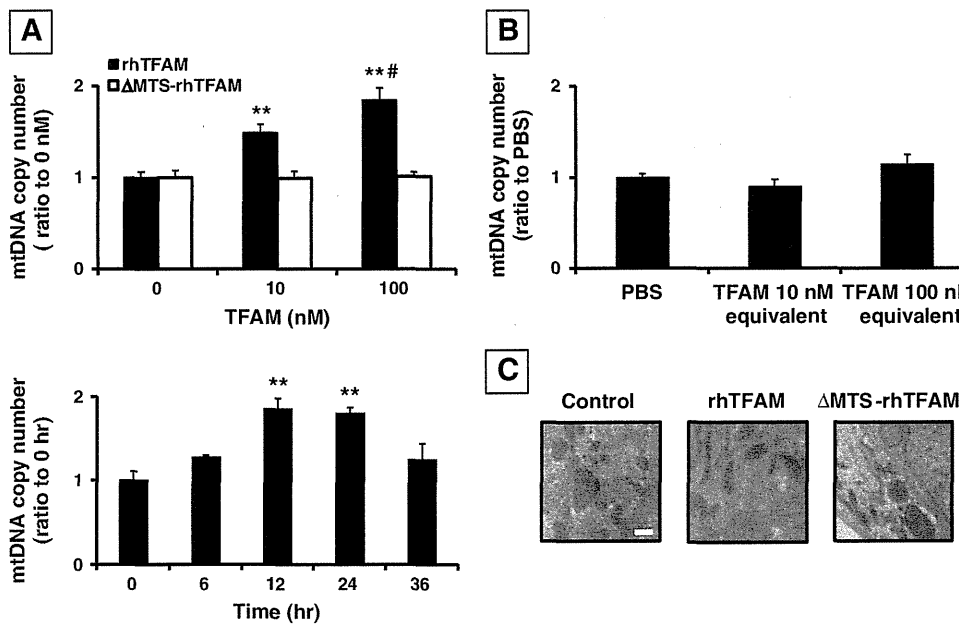

Fig. 3. The effects of rhTFAM on mitochondrial characteristics. (A) mtDNA copy number in myocytes treated with rhTFAM or ΔMTS-rhTFAM (0–100 nM) for 12 h, and rhTFAM (100 nM) for 0–36 h, quantified by real-time PCR relative to nucleus genome (ATIII gene). Data are presented as ratio to 0 nM or 0 h. **: $P<0.01$ vs. 0 nM or 0 h, #: $P<0.05$ vs. 10 nM. (B) mtDNA copy number of myocytes after the treatment with the product from empty vector. Myocytes were treated with the product from the empty vector by the equivalent volume of rhTFAM 10 or 100 nM, and mtDNA copy number was quantified. Data are shown as a ratio to buffer control (PBS). Values are mean ± SEM. (C) rhTFAM or ΔMTS-rhTFAM did not affect the morphology and number of mitochondria in cardiac myocytes, observed by TEM. Scale bar = 1 μm.

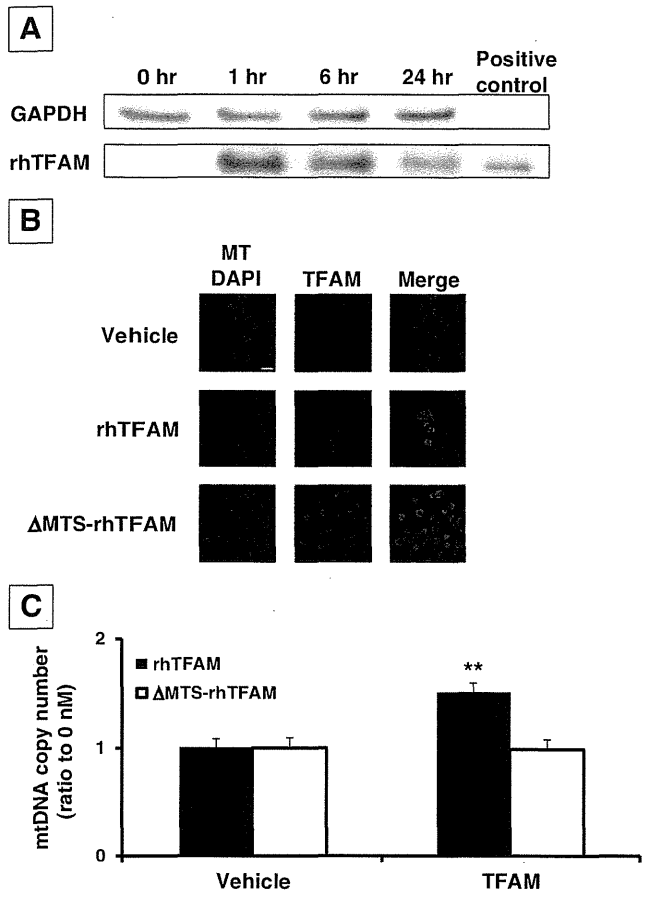

Fig. 4. The recruitment and function of rhTFAM on RAW 264.7 cells. (A) Western blot analysis of RAW 264.7 cells treated with rhTFAM protein for 0–24 h. (B) Confocal microscopic observations of RAW 264.7 cells treated with rhTFAM or ΔMTS-rhTFAM. Red represents mitochondria (MT), green represents human TFAM (Alexa Fluor 488), and blue represents nucleus (DAPI). Scale bar = 10 μm. (C) mtDNA copy number in RAW 264.7 cells treated with rhTFAM or ΔMTS-rhTFAM (50 nM) for 12 h, quantified by real-time PCR relative to nucleus genome (RPL27 gene). Data are presented as ratio to vehicle. **: $P<0.01$ vs. vehicle.

increased mtDNA-encoded COX I and COX III protein expression, which is a component of mitochondrial electron transport complex IV (Fig. 5A and B). In contrast, there were no increase of nuclear DNA-encoded NDUFA9 (complex I component) and SDHA (complex II component) protein contents (Fig. 5C and D). These results suggested that rhTFAM increased mtDNA copy number and subsequently increased mtDNA-encoded, but not nuclear DNA-encoded, mitochondrial proteins.

3.3. rhTFAM inhibited nuclear translocation of NFAT, NFAT transcriptional activity, and NFAT-dependent gene expression

Since overexpression of TFAM ameliorated post-MI remodeling in vivo, we expected rhTFAM also attenuated pathological hypertrophy and remodeling signals. The calcineurin/NFAT signaling pathway is a crucial signal that promotes pathological cardiac hypertrophy, both in vitro and in vivo (McKinsey and Kass, 2007; Molkentin, 2004; Vega et al., 2003). Dephosphorylation of NFAT by calcineurin, a Ca^{2+}-dependent serine/threonine phosphatase, induces cytosol-to-nucleus translocation, and NFAT functions as a transcriptional factor that activates many prohypertrophic genes. Furthermore, previous reports have suggested that the inhibition of NFAT signaling attenuated cardiac hypertrophy and failure (Sakata et al., 2000; van Rooij et al., 2004). We hypothesized that rhTFAM could also inhibit NFAT activation. We stimulated cardiac myocytes with AngII or ET-1, which are the major neurohumoral factors of pathological cardiac hypertrophy. First we investigated whether rhTFAM attenuated AngII- or ET-1-induced NFAT nuclear translocation using recombinant adenovirus encoding GFP-NFAT. The pretreatment with rhTFAM (100 nM) significantly inhibited AngII (100 nM)- or ET-1 (100 nM)-induced nuclear translocation of GFP-NFAT, whereas the pretreatment with ΔMTS-rhTFAM (100 nM) had no effect (Fig. 6A and B). This result suggested that recombinant TFAM recruited in mitochondria inhibited AngII- or ET-1-induced NFAT activation. Moreover, NFAT transcriptional activity as assessed by luciferase assay increased approximately 2.5-fold by stimulation with AngII (100 nM) or ET-1 (100 nM), and these increases were totally inhibited by the pretreatment with rhTFAM (10 nM) (Fig. 6C). The promoter activity of BNP gene, a NFAT-target gene widely used as marker of pathological cardiac hypertrophy, was also suppressed by rhTFAM (10 nM) (Fig. 6D). The expression of MCIP1 gene is also regulated by NFAT, and is used as a reporter gene of NFAT (Jin et al., 2010). MCIP1 mRNA expression was inhibited by the treatment with rhTFAM at baseline, just like TFAM-overexpression mice (Fig. 6E and F). These results confirmed that rhTFAM attenuated AngII- or ET-1-induced NFAT activation in cardiac myocytes.

We also investigated whether rhTFAM modulates MAPK p44/42 (ERK 1/2), another important pathway that induces cardiac hypertrophy (Aoki et al., 2000; McKinsey and Kass, 2007). The pretreatment with rhTFAM (100 nM) had no effect on ET-1 (100 nM)-induced MAPK p44/42 phosphorylation level (Fig. 7), suggesting that rhTFAM attenuates hypertrophy independent of MAPK signaling.

Since NFAT is regulated by the frequency of Ca^{2+} oscillation, we investigated the effect of rhTFAM on Ca^{2+} release from mitochondria. Stimulation with AngII (100 nM) or ET-1 (100 nM) decreased mitochondrial $[Ca^{2+}]$ in cardiac myocytes, and rhTFAM (10 nM) significantly suppressed these decrease (Fig. 8). This result suggested that rhTFAM suppressed AngII- or ET-1-induced Ca^{2+} release from mitochondria to cytoplasm.

3.4. rhTFAM attenuated pathological hypertrophy of cardiac myocytes

Finally we examined whether rhTFAM subsequently attenuates hypertrophic response of myocytes. The treatment with rhTFAM (10 nM) significantly reduced the hypertrophic reactions induced by the stimulation with AngII (100 nM) or ET-1 (100 nM) for 48 h (Fig. 9A–C). We concluded that rhTFAM attenuates AngII- or ET-1-induced hypertrophy of cardiac myocytes.

4. Discussion

In our previous report we showed that, after MI, the overexpression of TFAM attenuated the decrease of mtDNA copy number, ameliorated pathological hypertrophy and improved survival rate dramatically (Ikeuchi et al., 2005). Thus from the clinical point of view, our next interest was to find the strategy to increase TFAM or mtDNA copy number efficiently. Accordingly, this report has mainly two novel findings. First, this is the first report showing that rhTFAM protein is successfully recruited into mitochondria of cardiac myocytes, and functions to increase mtDNA copy number. The other finding is that rhTFAM inhibits NFAT signaling and consequently attenuates morphological remodeling of cardiac myocytes. These results will enable novel new strategy to increase mtDNA copy number and attenuate pathological cardiac hypertrophy.

4.1. The recruitment of rhTFAM into cardiac myocytes

Previously it has been reported that recombinant TFAM with protein transduction domain was entered into cultured cells (Iyer et al., 2009). This study is the first report that rhTFAM which has the almost

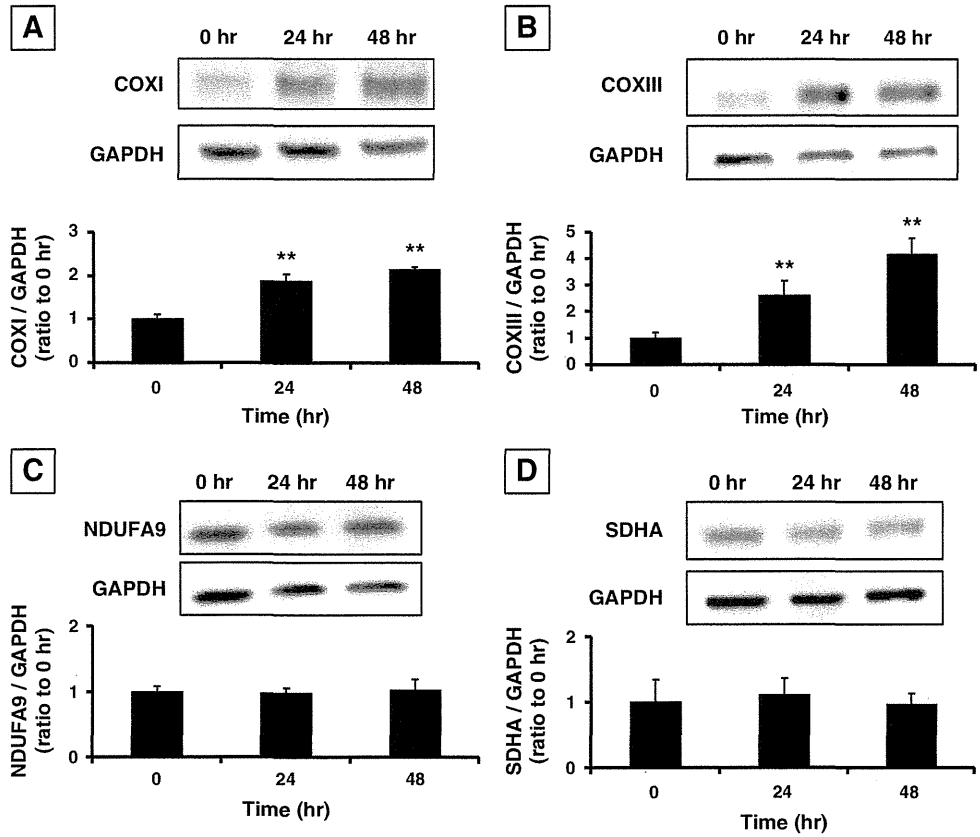

Fig. 5. The effects of rhTFAM on mitochondrial electron transport complex proteins. (A–D) The protein expression of COX I (A), COX III (B), NDUFA9 (C), and SDHA (D), 0–48 h after the treatment with rhTFAM. Data are presented as ratio to 0 h. **: $P<0.01$ vs. 0 h. Values are mean ± SEM.

identical amino acid sequence with native human TFAM can be successfully recruited into cardiac myocytes. Our result that rhTFAM-ΔC did not recruit into cells suggests that C-terminal tail of TFAM is responsible for this interesting property. Furthermore, we confirmed the recruitment and function of rhTFAM are independent of the cell types. The mechanism of its recruitment into cardiac myocytes remains unknown. Our data that rhTFAM entered into cells as early as 10 min, which was not inhibited in low temperature nor endocytosis inhibitors (data not shown), provides possibility that rhTFAM recruited into cytosol by a receptor-mediated pathway. Further investigations for the identification of the pathways for the recruitment of recombinant TFAM into the cells are necessary.

4.2. The effect of rhTFAM on mitochondrial characteristics

rhTFAM increased mtDNA copy number in myocytes (Fig. 3A) in a dose-dependent manner. Other than functioning as a transcription factor, endogenous TFAM regulates the amount of mtDNA by stabilizing mtDNA by forming a nucleoid structure (Kang et al., 2007). Considering the previous finding that the amount of mtDNA changes corresponding to the amount of TFAM, our results suggest that exogenously administered rhTFAM functioned similarly just like endogenous TFAM (Kanki et al., 2004). Furthermore, since ΔMTS-rhTFAM entered into myocytes but did not increase mtDNA copy number, it is likely that rhTFAM that entered mitochondria increased mtDNA copies. In this study, the mtDNA copy number peaked at 12 to 24 h after the rhTFAM treatment, and declined gradually thereafter. A single treatment with rhTFAM in myocytes prior to AngII or ET-1 stimulation successfully ameliorated pathological remodeling signals and subsequent pathological hypertrophy.

rhTFAM increased mtDNA-encoded, but not nuclear-encoded, mitochondrial proteins (Fig. 5). Probably it will be because of the increased mtDNA copy number, which is consistent with other's previous report that recombinant TFAM with protein transduction domain increased mitochondrial electron transport function and ATP synthesis in cultured cells (Thomas et al., 2011).

4.3. The effect of rhTFAM on NFAT signaling and pathological hypertrophy

The treatment with rhTFAM inhibited NFAT signaling in cardiac myocytes, and subsequent gene expression of MCIP1, which is a downstream of NFAT signaling, as well as in TFAM-overexpression mice hearts (Fig. 6E and F). The mechanism how rhTFAM inhibited AngII or ET-1-induced NFAT activation and hypertrophic response remains unknown. We need further investigation about the precise mechanism. Since mitochondria is known to participate in intracellular Ca^{2+} homeostasis via several Ca^{2+} uptake and release pathways (Bernardi, 1999), we speculated that rhTFAM inhibited Ca^{2+}/calcineurin-NFAT signaling by modulating $[Ca^{2+}]$. In fact, AngII or ET-1 induced the decrease of mitochondrial $[Ca^{2+}]$, suggesting the increase of Ca^{2+} release from mitochondria to cytoplasm, and rhTFAM inhibited AngII or ET-1-induced decrease of mitochondrial $[Ca^{2+}]$ (Fig. 8). However, the mechanism how rhTFAM inhibited AngII or ET-1-induced mitochondrial Ca^{2+} release still remains unknown. AngII is known to increase mitochondrial ROS in cardiac myocytes (Dai et al., 2011a, 2011b), and increased mitochondrial ROS is associated with mitochondrial Ca^{2+} release from mitochondria to cytoplasm (Kalivendi et al., 2005). rhTFAM inhibited superoxide production induced by rotenone, a complex I inhibitor, in cardiac myocytes (data not shown). Accordingly, the impact of rhTFAM on mitochondrial $[Ca^{2+}]$ might be associated with the inhibition of excessive mitochondrial ROS generation.

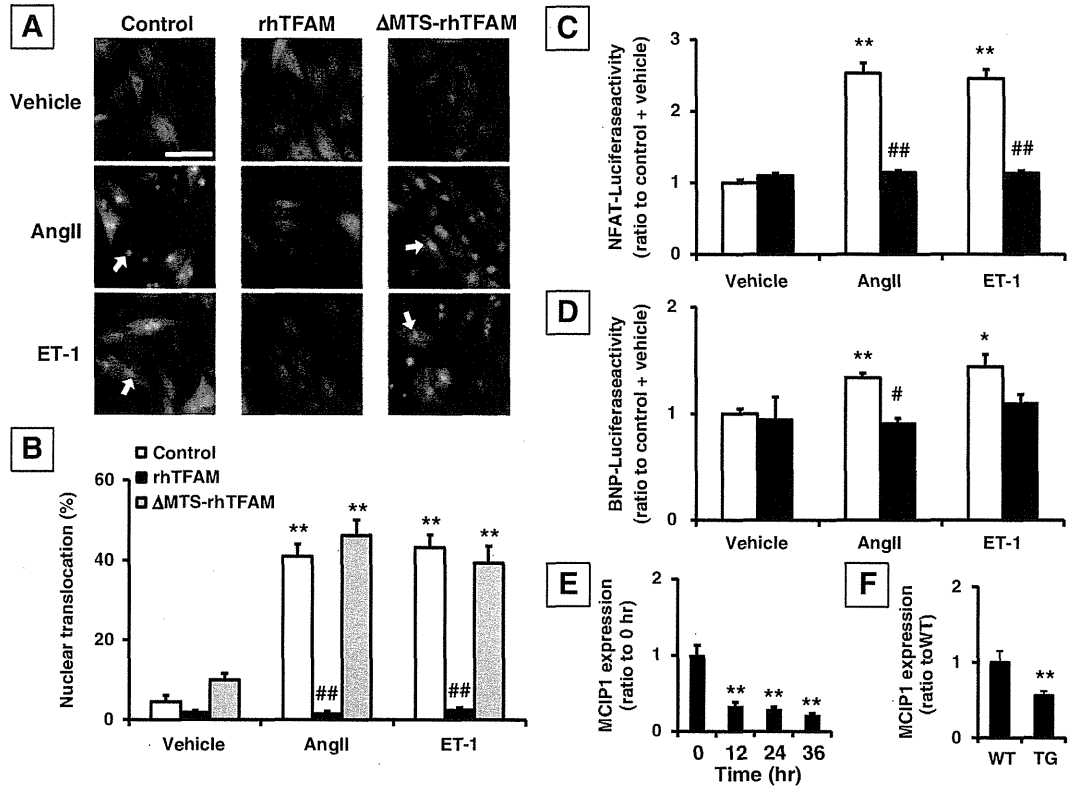

Fig. 6. The effects of rhTFAM on NFAT signaling. (A) The localization of GFP-NFAT protein in cardiac myocytes after the stimulation with AngII or ET-1. Arrows show GFP-NFAT translocated to nucleus. Scale bar = 50 μm. (B) rhTFAM significantly reduced the nuclear translocation rate of GFP-NFAT, whereas ΔMTS-rhTFAM had no effect on this translocation. (C and D) NFAT-luciferase activity (C) and BNP-luciferase activity (D) of myocytes stimulated with AngII or ET-1. NFAT- and BNP-luciferase activities were quantified as ratios to SV40 luciferase activity. Data are presented as ratio to control + vehicle. **: $P<0.01$, *: $P<0.05$ vs. control + vehicle; ##: $P<0.01$, #: $P<0.05$ vs. control. (E) MCIP1 mRNA expression in cardiac myocytes, 0–36 h after the treatment with rhTFAM. Data are presented as ratio to 0 h. **: $P<0.01$ vs. 0 h. (F) Cardiac MCIP1 mRNA expression of TFAM-overexpression mice and wild type littermates ($n=5$). WT means wild type mice, and TG means TFAM-overexpression mice. **: $P<0.01$ vs. WT. Values are mean ± SEM.

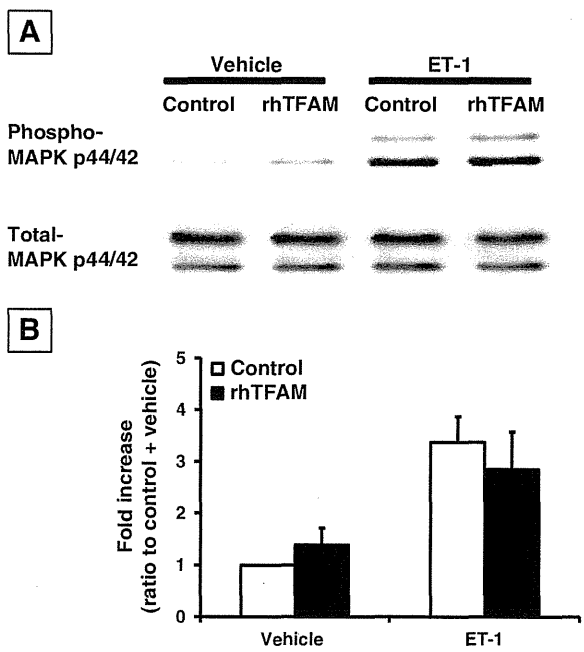

Fig. 7. The effects of rhTFAM on phosphorylation of MAPK p44/42. (A) Western blot analysis of myocytes probed with phospho-specific antibody and then reprobed for total protein. (B) The quantification of the ratio of phospho- to total-MAPK p44/42. The values were normalized to control + vehicle, and the data are shown as ratio to control + vehicle. Values are mean ± SEM.

NFAT signaling participates in pathological but not in physiological hypertrophy (Wilkins et al., 2004). Although hypertrophy has been traditionally viewed as a necessary first response to pathological stress but only later exacerbates disease, recent data suggest that hypertrophy in response to pathological stress may never be truly adaptive, and clinical studies support benefits from its inhibition (Frey et al., 2004; Gardin and Lauer, 2004; McKinsey and Kass, 2007). Moreover, the inhibition of NFAT signaling is reported to attenuate cardiac hypertrophy and failure (Sakata et al., 2000; van Rooij et al., 2004). Taken together, we believe that inhibiting NFAT signaling using rhTFAM can prevent cardiac hypertrophy and lead to the prevention of heart failure. We need further investigation, especially in vivo experiments, to confirm rhTFAM inhibits pathological cardiac hypertrophy and failure.

A possibility still exist that rhTFAM affected on other pathways besides NFAT signaling and subsequently inhibited AngII- or ET-1-induced hypertrophy of cardiac myocytes. However, we conclude in this study that exogenous rhTFAM have potential to increase mtDNA and inhibit pathological NFAT signaling in myocytes. Further elucidation of the precise mechanisms that TFAM functions in failing myocardium will be necessary.

5. Clinical implications

We propose in this report extreme novel findings that exogenously administered rhTFAM increased mtDNA copy number and attenuated pathological hypertrophy of cardiac myocytes. Thus rhTFAM could be a novel clinical strategy to increase mtDNA copy number and subsequently inhibit cardiac hypertrophy and failure. Further investigations of rhTFAM are anticipated.

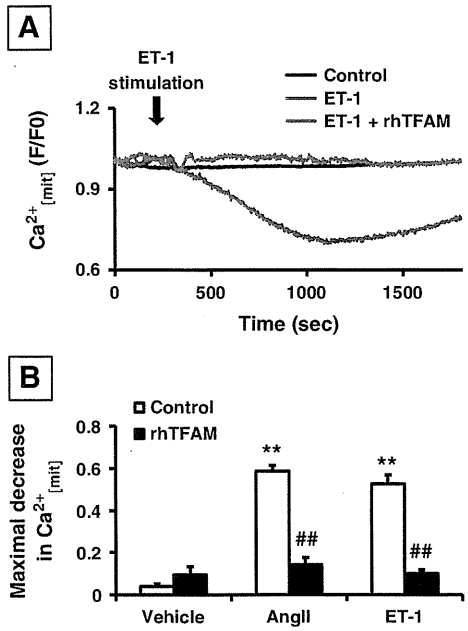

Fig. 8. The effects of rhTFAM on mitochondrial [Ca^{2+}]. (A) Representative trace of mitochondrial [Ca^{2+}] after the stimulation with ET-1, visualized using rhod-2. (B) rhTFAM significantly attenuated AngII- or ET-1-induced decrease of mitochondrial [Ca^{2+}]. **: $P<0.01$ vs. control + vehicle, ##: $P<0.01$ vs. control. Values are mean ± SEM.

Funding

This work was supported by Grant-in-Aid for Scientific Research (S) (23220013) and for Scientific Research (C) (23591084) from the Japan Society for the Promotion of Science.

Disclosures

None.

Acknowledgements

We thank Ms. Michiyo Tanaka for technical assistant. We appreciate the technical support from the Research Support Center, Graduate School of Medical Sciences, Kyushu University.

References

Alam, T.I., Kanki, T., Muta, T., Ukaji, K., Abe, Y., Nakayama, H., Takio, K., Hamasaki, N., Kang, D., 2003. Human mitochondrial DNA is packaged with TFAM. Nucleic Acids Res. 31, 1640–1645.

Aoki, H., Richmond, M., Izumo, S., Sadoshima, J., 2000. Specific role of the extracellular signal-regulated kinase pathway in angiotensin II-induced cardiac hypertrophy in vitro. Biochem. J. 347 (Pt 1), 275–284.

Bernardi, P., 1999. Mitochondrial transport of cations: channels, exchangers, and permeability transition. Physiol. Rev. 79, 1127–1155.

Dai, D.F., Chen, T., Szeto, H., Nieves-Cintron, M., Kutyavin, V., Santana, L.F., Rabinovitch, P.S., 2011a. Mitochondrial targeted antioxidant peptide ameliorates hypertensive cardiomyopathy. J. Am. Coll. Cardiol. 58, 73–82.

Dai, D.F., Johnson, S.C., Villarin, J.J., Chin, M.T., Nieves-Cintron, M., Chen, T., Marcinek, D.J., Dorn II, G.W., Kang, Y.J., Prolla, T.A., Santana, L.F., Rabinovitch, P.S., 2011b. Mitochondrial oxidative stress mediates angiotensin II-induced cardiac hypertrophy and Galphaq overexpression-induced heart failure. Circ. Res. 108, 837–846.

Frey, N., Katus, H.A., Olson, E.N., Hill, J.A., 2004. Hypertrophy of the heart: a new therapeutic target? Circulation 109, 1580–1589.

Fujii, T., Onohara, N., Maruyama, Y., Tanabe, S., Kobayashi, H., Fukutomi, M., Nagamatsu, Y., Nishihara, N., Inoue, R., Sumimoto, H., Shibasaki, F., Nagao, T., Nishida, M., Kurose, H., 2005. Galpha12/13-mediated production of reactive oxygen species is critical for angiotensin receptor-induced NFAT activation in cardiac fibroblasts. J. Biol. Chem. 280, 23041–23047.

Gardin, J.M., Lauer, M.S., 2004. Left ventricular hypertrophy: the next treatable, silent killer? JAMA 292, 2396–2398.

Garnier, A., Fortin, D., Delomenie, C., Momken, I., Veksler, V., Ventura-Clapier, R., 2003. Depressed mitochondrial transcription factors and oxidative capacity in rat failing cardiac and skeletal muscles. J. Physiol. 551, 491–501.

Hayashi, Y., Yoshida, M., Yamato, M., Ide, T., Wu, Z., Ochi-Shindou, M., Kanki, T., Kang, D., Sunagawa, K., Tsutsui, H., Nakanishi, H., 2008. Reverse of age-dependent

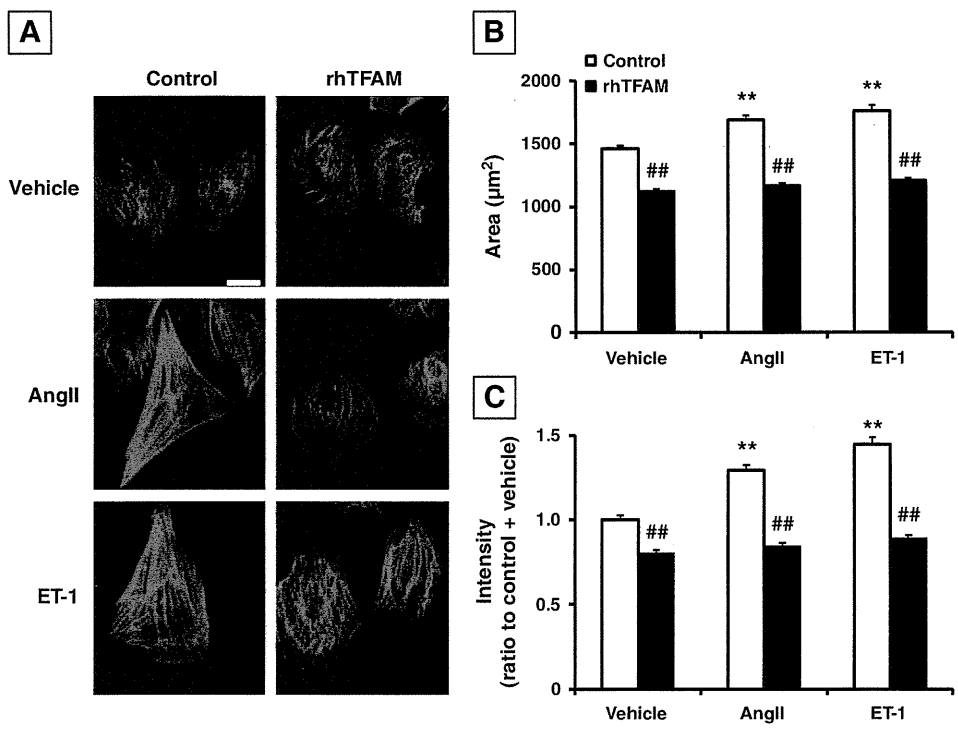

Fig. 9. Morphological remodeling of cardiac myocytes stimulated with AngII or ET-1. (A) Representative photomicrographs of AngII- or ET-1-stimulated myocytes immunostained using phalloidin. Scale bar = 20 μm. (B and C) Mean cell surface area (B) and fluorescent intensity (C) of 200–250 cells. **: $P<0.01$ vs. control + vehicle, ##: $P<0.01$ vs. control. Values are mean ± SEM.

memory impairment and mitochondrial DNA damage in microglia by an overexpression of human mitochondrial transcription factor a in mice. J. Neurosci. 28, 8624–8634.
Ide, T., Tsutsui, H., Hayashidani, S., Kang, D., Suematsu, N., Nakamura, K., Utsumi, H., Hamasaki, N., Takeshita, A., 2001. Mitochondrial DNA damage and dysfunction associated with oxidative stress in failing hearts after myocardial infarction. Circ. Res. 88, 529–535.
Ikeuchi, M., Matsusaka, H., Kang, D., Matsushima, S., Ide, T., Kubota, T., Fujiwara, T., Hamasaki, N., Takeshita, A., Sunagawa, K., Tsutsui, H., 2005. Overexpression of mitochondrial transcription factor a ameliorates mitochondrial deficiencies and cardiac failure after myocardial infarction. Circulation 112, 683–690.
Iyer, S., Thomas, R.R., Portell, F.R., Dunham, L.D., Quigley, C.K., Bennett Jr., J.P., 2009. Recombinant mitochondrial transcription factor A with N-terminal mitochondrial transduction domain increases respiration and mitochondrial gene expression. Mitochondrion 9, 196–203.
Jin, H., Hadri, L., Palomeque, J., Morel, C., Karakikes, I., Kaprielian, R., Hajjar, R., Lebeche, D., 2010. KChIP2 attenuates cardiac hypertrophy through regulation of Ito and intracellular calcium signaling. J. Mol. Cell. Cardiol. 48, 1169–1179.
Kalivendi, S.V., Konorev, E.A., Cunningham, S., Vanamala, S.K., Kaji, E.H., Joseph, J., Kalyanaraman, B., 2005. Doxorubicin activates nuclear factor of activated T-lymphocytes and Fas ligand transcription: role of mitochondrial reactive oxygen species and calcium. Biochem. J. 389, 527–539.
Kang, D., Kim, S.H., Hamasaki, N., 2007. Mitochondrial transcription factor A (TFAM): roles in maintenance of mtDNA and cellular functions. Mitochondrion 7, 39–44.
Kanki, T., Ohgaki, K., Gaspari, M., Gustafsson, C.M., Fukuoh, A., Sasaki, N., Hamasaki, N., Kang, D., 2004. Architectural role of mitochondrial transcription factor A in maintenance of human mitochondrial DNA. Mol. Cell. Biol. 24, 9823–9834.
Karamanlidis, G., Nascimben, L., Couper, G.S., Shekar, P.S., del Monte, F., Tian, R., 2010. Defective DNA replication impairs mitochondrial biogenesis in human failing hearts. Circ. Res. 106, 1541–1548.
Lagouge, M., Argmann, C., Gerhart-Hines, Z., Meziane, H., Lerin, C., Daussin, F., Messadeq, N., Milne, J., Lambert, P., Elliott, P., Geny, B., Laakso, M., Puigserver, P., Auwerx, J., 2006. Resveratrol improves mitochondrial function and protects against metabolic disease by activating SIRT1 and PGC-1alpha. Cell 127, 1109–1122.
Larsson, N.G., Wang, J., Wilhelmsson, H., Oldfors, A., Rustin, P., Lewandoski, M., Barsh, G.S., Clayton, D.A., 1998. Mitochondrial transcription factor A is necessary for mtDNA maintenance and embryogenesis in mice. Nat. Genet. 18, 231–236.
Li, H., Wang, J., Wilhelmsson, H., Hansson, A., Thoren, P., Duffy, J., Rustin, P., Larsson, N.G., 2000. Genetic modification of survival in tissue-specific knockout mice with mitochondrial cardiomyopathy. Proc. Natl. Acad. Sci. U. S. A. 97, 3467–3472.
McKinsey, T.A., Kass, D.A., 2007. Small-molecule therapies for cardiac hypertrophy: moving beneath the cell surface. Nat. Rev. Drug Discov. 6, 617–635.
Molkentin, J.D., 2004. Calcineurin-NFAT signaling regulates the cardiac hypertrophic response in coordination with the MAPKs. Cardiovasc. Res. 63, 467–475.
Nishida, M., Onohara, N., Sato, Y., Suda, R., Ogushi, M., Tanabe, S., Inoue, R., Mori, Y., Kurose, H., 2007. Galpha12/13-mediated up-regulation of TRPC6 negatively regulates endothelin-1-induced cardiac myofibroblast formation and collagen synthesis through nuclear factor of activated T cells activation. J. Biol. Chem. 282, 23117–23128.
Nishida, M., Watanabe, K., Sato, Y., Nakaya, M., Kitajima, N., Ide, T., Inoue, R., Kurose, H., 2010. Phosphorylation of TRPC6 channels at Thr69 is required for anti-hypertrophic effects of phosphodiesterase 5 inhibition. J. Biol. Chem. 285, 13244–13253.
Ohgaki, K., Kanki, T., Fukuoh, A., Kurisaki, H., Aoki, Y., Ikeuchi, M., Kim, S.H., Hamasaki, N., Kang, D., 2007. The C-terminal tail of mitochondrial transcription factor a markedly strengthens its general binding to DNA. J. Biochem. 141, 201–211.
Parisi, M.A., Clayton, D.A., 1991. Similarity of human mitochondrial transcription factor 1 to high mobility group proteins. Science 252, 965–969.
Sakata, Y., Masuyama, T., Yamamoto, K., Nishikawa, N., Yamamoto, H., Kondo, H., Ono, K., Otsu, K., Kuzuya, T., Miwa, T., Takeda, H., Miyamoto, E., Hori, M., 2000. Calcineurin inhibitor attenuates left ventricular hypertrophy, leading to prevention of heart failure in hypertensive rats. Circulation 102, 2269–2275.
Thomas, R.R., Khan, S.M., Portell, F.R., Smigrodzki, R.M., Bennett Jr., J.P., 2011. Recombinant human mitochondrial transcription factor A stimulates mitochondrial biogenesis and ATP synthesis, improves motor function after MPTP, reduces oxidative stress and increases survival after endotoxin. Mitochondrion 11, 108–118.
Tsutsumi, T., Ide, T., Yamato, M., Kudou, W., Andou, M., Hirooka, Y., Utsumi, H., Tsutsui, H., Sunagawa, K., 2008. Modulation of the myocardial redox state by vagal nerve stimulation after experimental myocardial infarction. Cardiovasc. Res. 77, 713–721.
van Rooij, E., Doevendans, P.A., Crijns, H.J., Heeneman, S., Lips, D.J., van Bilsen, M., Williams, R.S., Olson, E.N., Bassel-Duby, R., Rothermel, B.A., De Windt, L.J., 2004. MCIP1 overexpression suppresses left ventricular remodeling and sustains cardiac function after myocardial infarction. Circ. Res. 94, e18–e26.
Vega, R.B., Rothermel, B.A., Weinheimer, C.J., Kovacs, A., Naseem, R.H., Bassel-Duby, R., Williams, R.S., Olson, E.N., 2003. Dual roles of modulatory calcineurin-interacting protein 1 in cardiac hypertrophy. Proc. Natl. Acad. Sci. U. S. A. 100, 669–674.
Wang, J., Wilhelmsson, H., Graff, C., Li, H., Oldfors, A., Rustin, P., Bruning, J.C., Kahn, C.R., Clayton, D.A., Barsh, G.S., Thoren, P., Larsson, N.G., 1999. Dilated cardiomyopathy and atrioventricular conduction blocks induced by heart-specific inactivation of mitochondrial DNA gene expression. Nat. Genet. 21, 133–137.
Wilkins, B.J., Dai, Y.S., Bueno, O.F., Parsons, S.A., Xu, J., Plank, D.M., Jones, F., Kimball, T.R., Molkentin, J.D., 2004. Calcineurin/NFAT coupling participates in pathological, but not physiological, cardiac hypertrophy. Circ. Res. 94, 110–118.

International Journal of Cardiology xxx (2012) xxx–xxx

Contents lists available at SciVerse ScienceDirect

International Journal of Cardiology

journal homepage: www.elsevier.com/locate/ijcard

Letter to the Editor

Screening for Fabry disease in patients with left ventricular hypertrophy ☆

Kazutoshi Mawatari [a], Hideo Yasukawa [a,*], Toyoharu Oba [a], Takanobu Nagata [a], Tadayasu Togawa [c], Takahiro Tsukimura [c], Sachiko Kyogoku [a], Hideki Ohshima [a], Tomoko Minami [a], Yusuke Sugi [a], Hitoshi Sakuraba [c,d], Tsutomu Imaizumi [a,b]

[a] Division of Cardiovascular Medicine, Department of Internal Medicine, Kurume University School of Medicine, 67 Asahi-machi, Kurume 830-0011, Japan
[b] Cardiovascular Research Institute, Kurume University, 67 Asahi-machi, Kurume 830-0011, Japan
[c] Department of Analytical Biochemistry, Meiji Pharmaceutical University, 2-522-1 Noshio, Kiyose, Tokyo 204-8588, Japan
[d] Department of Clinical Genetics, Meiji Pharmaceutical University, 2-522-1 Noshio, Kiyose, Tokyo 204-8588, Japan

ARTICLE INFO

Article history:
Received 27 September 2012
Accepted 28 October 2012
Available online xxxx

Keywords:
Fabry disease
α-Galactosidase A
Left ventricular hypertrophy
Functional polymorphism
E66Q

Fabry disease (OMIM 301500) is a rare heritable X-linked lysosomal storage disorder that is caused by a deficient activity of the enzyme α-galactosidase A (α-GAL) enzyme [1]. This enzyme defect leads to progressive accumulation of glycosphingolipids such as globotriaosylceramide (Gb3) in a wide variety of tissues including vascular endothelium, renal glomeruli and tubules, cardiac myocytes, conducting tissue and valves, and skin, eventually impairing organ function [2]. Clinical features of classic Fabry disease include proteinuria, progressive renal impairment, left ventricular hypertrophy (LVH), conduction abnormalities, hypohidrosis, painful paresthesia of the hands and feet (acroparesthesia), and vascular skin lesions (angiokeratoma) [1–3].

The prevalence of Fabry disease has been reported to range from 1 in 117,000 to 1 in 40,000 live births [1–3]. Higher prevalences of Fabry disease have been reported in high-risk populations, such as dialysis patients or patients with LVH. In addition to classic Fabry disease, a variant form, cardiac Fabry disease, manifests mainly as LVH without other organ involvement [4]. Several investigators have reported the prevalence of cardiac Fabry disease as ranging from 0 to 12% of patients with LVH [5–12]. Since LVH is one of the main clinical manifestations of Fabry disease and enzyme replacement therapy with recombinant human α-GAL has been available to attenuate LVH [13], screening and definite diagnosis of this disease are clinically very important.

A total of 738 male patients with LVH (maximal left ventricle wall ≥ 13 mm on echocardiography) were enrolled in this study from 25 clinical facilities in the southwest area of Japan (Kyushu Island). This study was approved by the ethics committee of Kurume University. Written informed consent was obtained from each patient. The authors of this manuscript have certified that they comply with the Principles of Ethical Publishing in the International Journal of Cardiology [14]. Serum α-GAL activity was measured with a fluorometric enzyme assay as previously described [15]. When serum α-GAL activity was lower than 1.5 nmol/h/m, the leukocyte α-GAL activity was also measured.

Fig. 1 shows the distribution of serum α-GAL activities in these subjects. The average of the serum α-GAL activities in all the subjects was 4.8 nmol/h/mL (SD 1.4 nmol/h/mL). Four patients exhibited serum α-GAL activity lower than 1.5 nmol/h/mL, the cut-off value previously described [15]. These four patients with LVH were measured for leukocyte α-GAL activity. Three of the four first screen-positive subjects (Table 1, Subjects 1–3) had low but measurable

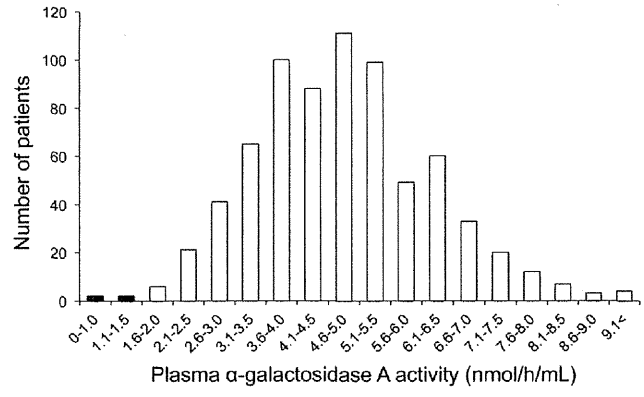

Fig. 1. Distribution of serum α-galactosidase A activity in all patients with left ventricular hypertrophy (n=738). The mean value was 4.8 nmol/h/mL (SD 1.4 nmol/h/mL).

☆ Source of funding: This study was supported in part by a grant from the Science Frontier Research Promotion Centers (Cardiovascular Research Institute); by Grants-in-Aid for Scientific Research (HY, TI) from the Ministry of Education, Science, Sports, and Culture, Japan; and by a Japanese Ministry of Health, Labour and Welfare Research Grants (TI).

* Corresponding author at: Division of Cardiovascular Medicine, Department of Internal Medicine, Cardiovascular Research Institute, Kurume University School of Medicine, 67 Asahi-machi, Kurume 830-0011, Japan. Tel.: +81 942 31 7562; fax: +81 942 33 6509.
E-mail address: yahideo@med.kurume-u.ac.jp (H. Yasukawa).

0167-5273/$ – see front matter © 2012 Published by Elsevier Ireland Ltd.
http://dx.doi.org/10.1016/j.ijcard.2012.10.076

Table 1
Clinical characteristics of patients with low plasma α-GAL activity.

Subject numbers	1	2	3	4
Age in years	68	86	92	48
Clinical diagnosis	HHD	HCM	HCM	HCM
Hypertension	+	−	−	+
Arrhythmia	−	AF	AF	−
Maximal left ventricular wall thickness in mm	13	14	17	17
Pattern of LVH	Concentric	Concentric	Concentric	ASH
Urinalysis	Proteinuria	Proteinuria	Normal	Normal
Stroke	−	−	Lacunar	−
Hypohidrosis	−	−	−	−
Limb pain	−	−	−	−
Plasma α-GAL activity (nmol/h/mL)	1.5	0.4	1.3	1
Leukocyte α-GAL activity (nmol/h/mg protein)	19	9	22	35
α-GAL gene mutation	E66Q	E66Q	E66Q	

α-GAL, α-galactosidase A; HHD, hypertensive heart disease; HCM, hypertrophic cardiomyopathy; LVH, left ventricular hypertrophy; AF, atrial fibrillation; ASH, asymmetric septal hypertrophy.

residual leukocyte α-GAL activity (18–45% of the normal control mean). For the three LVH subjects with moderately reduced leukocyte α-GAL activity, direct sequencing of seven exons of the gene encoding α-GAL was performed. All three patients harbored a G to C transition at position 196 in exon 2, leading to an amino-acid substitution from glutamic acid to glutamine at position 66 (E66Q).

We limited our study enrollment to male because Fabry heterozygous females exhibit a wide range of α-GAL activity, from extremely decreased to normal, according to the characteristics of an X-linked genetic disease [1,16]. Available data regarding the prevalence of cardiac Fabry disease, a variant form of Fabry disease that mainly manifests as LVH without other typical features of Fabry disease, are limited and controversial [3,5–12]. The first reported prevalence of cardiac Fabry disease was 3% among 230 subjects with LVH [3]. Two later studies of small cohorts reported higher prevalences of cardiac Fabry disease in male (6%) and female (12%) subjects with late onset hypertrophic cardiomyopathy [5,6]. In contrast, two other small cohort studies detected no cases of cardiac Fabry disease among subjects with hypertrophic cardiomyopathy [7,11]. Large-scale recent studies reported a 0.5–1.0% prevalence of cardiac Fabry disease in subjects with cardiac hypertrophy [8–10]. There are several possible reasons for the reported variations in the prevalence of cardiac Fabry disease. The prevalence may be dependent on the region screened, the cohort size, the method of screening, and the inclusion criteria for each study. Our cohort was located geographically near the previous cohort with a high prevalence of Fabry disease [3], the size of our cohort was large enough, and our inclusion criterion was similar to those of other studies [3,5,11]. In this study, we identified three patients with low but residual α-GAL activity, but no subjects in our cohort were deficient for enzyme activity (Fig. 2).

To date, more than 500 disease-causing mutations have been identified in the gene encoding α-GAL, as well as several functional polymorphisms [1,2]. Some of the latter were previously believed to be pathogenic, but are now recognized to be functional polymorphisms [15,17,18]. The E66Q mutation was also originally considered to be pathogenic, causing a variant form of Fabry disease, and patients with the E66Q mutation were treated with enzyme replacement therapy [3,19]. However, recent reports have suggested that E66Q mutation could instead be a functional polymorphism for the following reasons. The predicted structural change in α-GAL caused by E66Q substitution is small and localized far from both the active site and the dimer interface, which are critical for the enzyme activity of α-GAL [17,20]. Subjects harboring E66Q have leukocyte

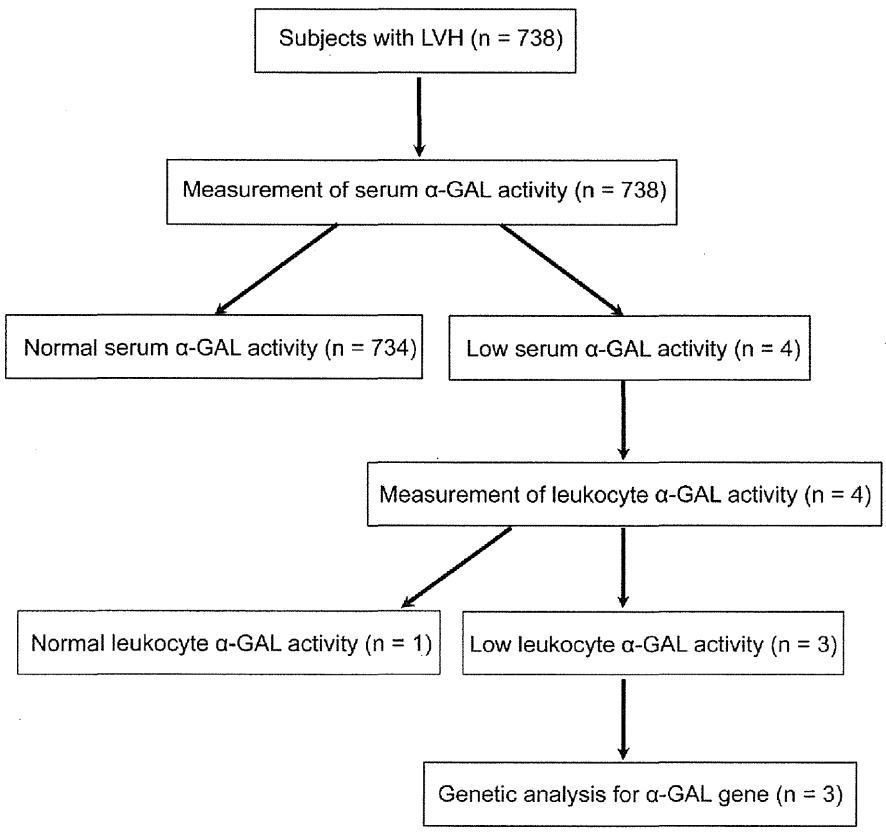

Fig. 2. Flow chart for the screening of patients with left ventricular hypertrophy for Fabry disease.

Please cite this article as: Mawatari K, et al, Screening for Fabry disease in patients with left ventricular hypertrophy, Int J Cardiol (2012), http://dx.doi.org/10.1016/j.ijcard.2012.10.076

α-GAL activities of ~24–65% of the normal control mean, although Fabry patients with pathogenic mutations exhibit little or no α-GAL activity. No accumulation of the globotriaosylceramide (Gb3) was previously observed in cultured skin fibroblasts from E66Q patients [17]. Electron microscopy of the biopsied skin tissues from a male subject harboring the E66Q substitution revealed no pathological changes specific to Fabry disease [17]. The nucleotide change causing E66Q has been found in screens for Fabry disease in Japanese male hemodialysis patients who do not manifest Fabry disease [15]. Lastly and importantly, the reported allele frequency of the E66Q substitution was 1% in the normal Korean population [19]. Taken together, these observations underlie the status of E66Q substitution as a functional polymorphism rather than a pathogenic mutation.

In conclusion, our data may indicate that the prevalence of cardiac Fabry disease is quite low in patients with LVH. Further, a definite diagnosis of Fabry disease requires analysis of the gene encoding α-GAL to exclude functional polymorphisms. We suggest that enzyme replacement therapy should be done only when a Fabry phenotype such as LVH is due to a mutation in the gene encoding α-GAL.

Acknowledgments

We thank all investigators who enrolled LVH patients in Kurume University Hospital and its affiliated hospitals. We also thank Kimiko Kimura, Miyuki Nishigata, Makiko Kiyohiro, and Miho Nakao for the excellent technical assistance.

References

[1] Yousef Z, Elliott PM, Cecchi F, et al. Left ventricular hypertrophy in Fabry disease: a practical approach to diagnosis. Eur Heart J 2012, http://dx.doi.org/10.1093/eurheartj/ehs166 [Epub ahead of print].
[2] Weidemann F, Niemann M, Warnock DG, et al. The Fabry cardiomyopathy: models for the cardiologist. Annu Rev Med 2011;62:59-67.
[3] Nakao S, Takenaka T, Maeda M, et al. An atypical variant of Fabry's disease in men with left ventricular hypertrophy. N Engl J Med 1995;333:288-93.
[4] von Scheidt W, Eng CM, Fitzmaurice TF, et al. An atypical variant of Fabry's disease with manifestations confined to the myocardium. N Engl J Med 1991;324:395-9.
[5] Sachdev B, Takenaka T, Teraguchi H, et al. Prevalence of Anderson–Fabry disease in male patients with late onset hypertrophic cardiomyopathy. Circulation 2002;105:1407-11.
[6] Chimenti C, Pieroni M, Morgante E, et al. Prevalence of Fabry disease in female patients with late-onset hypertrophic cardiomyopathy. Circulation 2004;110:1047-53.
[7] Ommen SR, Nishimura RA, Edwards WD. Fabry disease: a mimic for obstructive hypertrophic cardiomyopathy? Heart 2003;89:929-30.
[8] Elliott P, Baker R, Pasquale F, et al. Prevalence of Anderson–Fabry disease in patients with hypertrophic cardiomyopathy: the European Anderson–Fabry Disease survey. Heart 2011;97:1957-60.
[9] Hagège AA, Caudron E, Damy T, et al. FOCUS study investigators. Screening patients with hypertrophic cardiomyopathy for Fabry disease using a filter-paper test: the FOCUS study. Heart 2011;97:131-6.
[10] Monserrat L, Gimeno-Blanes JR, Marín F, et al. Prevalence of Fabry disease in a cohort of 508 unrelated patients with hypertrophic cardiomyopathy. J Am Coll Cardiol 2007;50:2399-403.
[11] Arad M, Maron BJ, Gorham JM, et al. Glycogen storage diseases presenting as hypertrophic cardiomyopathy. N Engl J Med 2005;352:362-72.
[12] Morita H, Larson MG, Barr SC, et al. Single-gene mutations and increased left ventricular wall thickness in the community: the Framingham Heart Study. Circulation 2006;113:2697-705.
[13] Mehta A, Beck M, Elliott P, et al. Fabry Outcome Survey investigators. Enzyme replacement therapy with agalsidase alfa in patients with Fabry's disease: an analysis of registry data. Lancet 2009;374:1986-96.
[14] Coats AJS, Shewan LG. Statement on authorship and publishing ethics in the International Journal of Cardiology. Int J Cardiol 2011;153:239-40.
[15] Doi K, Noiri E, Ishizu T, et al. High-throughput screening identified disease-causing mutants and functional variants of α-galactosidase A gene in Japanese male hemodialysis patients. J Hum Genet 2012, http://dx.doi.org/10.1038/jhg.2012.68 [Epub ahead of print].
[16] Linthorst GE, Bouwman MG, Wijburg FA, et al. Screening for Fabry disease in high-risk populations: a systematic review. J Med Genet 2010;47:217-22.
[17] Togawa T, Tsukimura T, Kodama T, et al. Fabry disease: biochemical, pathological and structural studies of the α-galactosidase A with E66Q amino acid substitution. Mol Genet Metab 2012;105:615-20.
[18] Yasuda M, Shabbeer J, Benson SD, et al. Fabry disease: characterization of alpha-galactosidase A double mutations and the D313Y plasma enzyme pseudodeficiency allele. Hum Mutat 2003;22:486-92.
[19] Yoshitama T, Nakao S, Takenaka T, et al. Molecular genetic, biochemical, and clinical studies in three families with cardiac Fabry's disease. Am J Cardiol 2001;87:71-5.
[20] Lee BH, Heo SH, Kim GH, et al. Mutations of the GLA gene in Korean patients with Fabry disease and frequency of the E66Q allele as a functional variant in Korean newborns. J Hum Genet 2010;55:512-7.

Please cite this article as: Mawatari K, et al, Screening for Fabry disease in patients with left ventricular hypertrophy, Int J Cardiol (2012), http://dx.doi.org/10.1016/j.ijcard.2012.10.076

Multidisciplinary Approach to Genome-Wide Association Study for Heart Failure Based on the Different Ethnicity

-An overview of the bioinformatics and a new concept of BWAS-

Teruhiko Toyo-oka[1)]*, Licht Toyo-oka[2)]*, Manfred Richter[3)], Toshihiro Tanaka[4)], Toshiaki Nakajima[5)], Sawa Kostin[3)]*, Toru Izumi[1)], Jutta Schaper[3)]* and Katsushi Tokunaga[2)]*

[1)]Department of Cardiovascular Medicine, Post-graduate School of Medicine, Kitasato University, [2)]Department of Human Genetics, Post-graduate School of Medicine, University of Tokyo, [3)]Department of Experimental Cardiology, Max-Planck Institute, Bad Nauheim, Germany, [4)]Laboratory for Cardiovascular Diseases, RIKEN, Yokohama, [5)] Department of Ischemic Circulatory Physiology, University of Tokyo, Japan.

*These authors equally contributed to the study.

A part of this report was presented as an introductory lecture of Albrecht Fleckenstein Award in the 17th International Congress of Heart Disease, Toronto, Canada, on July 29, 2012.

Present study was financially supported by the Research Grants from the Ministry of Education, Culture, Science and Sports, the Ministry of Health, Welfare and Labor, and the Motor Vehicle Foundation, Japan.

Correspondence to T. Toyo-oka, MD, PhD, Department of Cardiovascular Medicine, Post-graduate School of Medicine, Kitasato University, Japan. E-mail address to toyooka_2im@hotmail.com, fax address +81-3-3390-4322.

Preface

Heart failure (HF), a serious syndrome with diverse ethnicity and complicated etiology, is one of the leading causes of death. A part is heritable, though its underlying factors still remain elusive. GWAS (genome-wide association study) is promising for identifying the causative genes, directly or indirectly related genes as well as modifier genes that aggravate or ameliorate the clinical process to the advanced phase (1). This overview mainly focused our on-going HF-GWAS trial for the pathogenesis and/or progression of HF at the worldwide and whole genome levels, irrespective of the variable pathogenic factors common-in or specific-to different ethnicity, without missing biologically significant genes. We propose here a new concept of Bigenome (nuclear and mitochondrial)-Wide Association Study (BWAS) necessary for clarifying complexities of HF and providing therapeutic options.

Validity and Accuracy of a Case-Control Study

The case-control study has been defined as an observational epidemiological study of persons with the disease (or another outcome variable) of interest and "a suitable control group of persons without the disease (comparison group, reference group)". At a glance, it looks simple and persuasive but endogenously contains serious uncertainties. When in life-span? Under which circumstances and at where should be designated as the control group? What is "disease" or "normal"? Is it discernible to select candidate genes with majority rule? This paper aims not to discuss the medical determinism in case-control study but to realize an inevitable ambiguity to the principle of GWAS itself. The goal of GWAS targets identification of the potential, but often fuzzy gene(s), suggestive of a close or distant relationship to HF.

The current GWAS started as a post-genome project in Japan (Fig. 1). The genomic DNAs donated from the normal control and HF-cases and Affymetrix 6.0 for single nucleotide polymorphism (SNP)/single nucleotide variation (SNV)/ copy number variation (CNV) revealed ~1,500,000 haploid alterations and the

subsequent coding DNA sequence (CDS) analysis identified 7,287 SNPs with the χ^2 or Fisher's test. After restricting to the exons, or ORF, exon-intron border and stop codons, these SNPs reduced to ~1/3, consisting of 107 non-synonymous mutations, 54 stop codons, 23 insertion/ deletions (in/del) to cause frame shift and 2,688 synonymous mutations (Fig. 2). These mutants did not overlap with Caucasian patients with dilated cardiomyopathy (1). Various cases with HF were diagnosed with clinical symptoms, physiological, morphological, biochemical and/or serological features. Candidate genes included adhesion molecules, channel proteins, cell signaling, transcription factors, proteases and anonymous proteins and would be opened elsewhere.

Evaluation of p values after statistic tests and the Manhattan plot

The SNP prevalence rate was analyzed with statistic test and the p value of each SNP was calculated with appropriate statistics. For minor alleles, Fisher's test is favorable for the exact analysis than χ^2 test. The Manhattan plot, –log (p) along the physical site of each chromosome, showed a wide distribution (Fig. 3). Both sex-chromosomes and mt-genes were excluded from this report, because they include many candidates to be commented and require other algorithms to discuss the genetic background (2-5). Compared with previous report of the cumulative Manhattan plot of more than 100 GWAS reports (Fig. 3, A), present result revealed a sparse distribution between 6.90×10^{-165} and 9.82×10^{-5} (Fig. 3, B), requiring the increment of case number. Extremely high –log(p) values except MHC gene often represent gSNP (Fig. 3, B), not related to the pathogenicity. Also note that p values simply imply the statistic sureness and cannot be confused with the effect size that measures an influencing potential for the candidate genes.

Multiple Mutations in Each Nuclear Chromosome and Mitochondria

The mutation locus was not disseminated but scattered in each autosome with some concentrated bias on 1, 2, 5, 11, 13, 15, 19 and 22 chromosomes (Fig. 4). This fact may reflect natural selection under the *de novo*

mutation and suggests the biological ontology, *i.e.* drastic modification of the 2D/3D structure of the transcript or the transgene (4) may determine the viability or influence adoptability of mutants to environmental changes. These genetic modifications highlight the long-time mitochondrial (mt) symbiosis (5), because mt-genes often show heteroplasmy or ethnicity-dependent haplogroup. More than 90% of nuclear gene is occupied by introns, pseudogenes or synonymous mutations (Fig. 2). In contrast, mt-gene has own exons, tRNAs, rRNAs and much less non-coding region in d-loop. Combined mutation is useful for identifying the haplogroup (3-5). The mt-mutations in heart require careful evaluation, since polypeptide-coding exons or tRNAs play a pivotal role in the ATP synthesis, reactive oxygen species (ROS) production, apoptosis induction and/or HF (3, 4).

A Novel Concept, "Bigenome-Wide Association Study (BWAS)", and Conclusion

In addition to the nuclear gene, mt-gene also contributes to the incomparable pathophysiology at the cell/organ/body levels, particularly in muscular, cardiac and neural tissues (3) that require massive ATP. In addition to the nuclear gene, we intensify that mt-gene mutations should be considered along the time-course of HF and propose here a novel concept of Bigenome-Wide Association Study (BWAS), a combined research of nuclear and mt-genomes. This cross-talk between nuclear and mt-genes is different from the classic components located among mt-complexes coded by nuclear genes (NUMT, 3) and needed to maintain mt-function.

Our concept meant that multiple mutation in nuclear and mt-gene may aggravate HF age-dependently and synergistically *via* ROS formation, peroxidize adjacent constituents (DNAs, proteins or lipids), induce mutagenesis, reduce ATP production, enhance intracellular Ca^{2+} levels, decrease contractility of cardiac muscle cells, activate endogenous proteases (1) and result in apoptosis and/or necrosis (1, 3, 6). An interruption of these sequential events would produce the beneficial outcome of the patients with HF. Thus, we conclude that the gene analyses should be developed in both nuclear and mitochondrial levels to actualize the gene therapy.

References

1. Toyo-oka T, Kawada T, Nakata J, *et al.,* Translocation and cleavage of myocardial dystrophin as a common pathway to advanced heart failure: a scheme for the progression of cardiac dysfunction. *Proc Natl Acad Sci USA.* 101;7381-5, 2004.
2. Charchar FJ, Bloomer LD, Barnes TA, *et al.,* Inheritance of coronary artery disease in men: an analysis of the role of the Y chromosome. *Lancet* 379;915-22, 2012.
3. Wallace DC, Colloquium paper: bioenergetics, the origins of complexity, and the ascent of man. *Proc Natl Acad Sci USA* 107 (Suppl 2);8947-53, 2010.
4. Shin WS, Tanaka M, Suzuki J, *et al.,* A novel homoplasmic mutation in mtDNA with a single evolutionary origin as a risk factor for cardiomyopathy. *Am J Hum Genet.* 67;1617-20, 2000.
5. Toyo-oka T, Tanaka T, Toyo-oka L, *et al.,* In "*Genes and Cardiovascular Function*". Ostadal B. *et al.,* eds, Springer, pp85-92, 2011.
6. Toyo-oka T and Kumagai H. Cardiac troponin levels as a preferable biomarker of myocardial cell degradation. *Adv Exp Med Biol.* 592;241-9, 2007

Figure Legends

Fig. 1. Road-map to identify pathogenic SNPs related to HF.

Fig. 2. Gene distribution of SNPs in exom or open-reading frame (ORF) of HF. Note that total SNP number is determined by the threshold of p value.

Fig. 3. Accumulated Manhattan plots of >100 GWAS reported before (A) and HF-related SNP (B). Note that X-, Y-sex chromosomes and mt-gene contain the haplogroup linked to each algorithm (2, 5).

Fig. 4. Mutation numbers in each autosome indicating heterogeneous distribution of SNP.

Fig. 1

Case control study between HF and control Japanese

Microarray resequencing (900k) analysis → 909,14 3 alleles

↓

Additional RIKEN + TUH database → +10,660 alleles

↓

Squeezing with χ^2 analysis → 7,287 alleles with p values < 10^{-4}
p = 6.90E-165 ~ 9.82E-5

↓

Exclusion of solitary intron SNPs not belonging to any coding gene → 2,872 loci

↓

Identification of missense or non-sense mutations → 107 non-synony. mutations
54 stop codons
23 in/del
(2,688 synonymous mutations)

↓

Pathophysiological significance employing multidiciplanary approaches → 2D/3D structure, immunostaining, crystallography, biological activity, transgenic animals *etc.*

Fig. 2

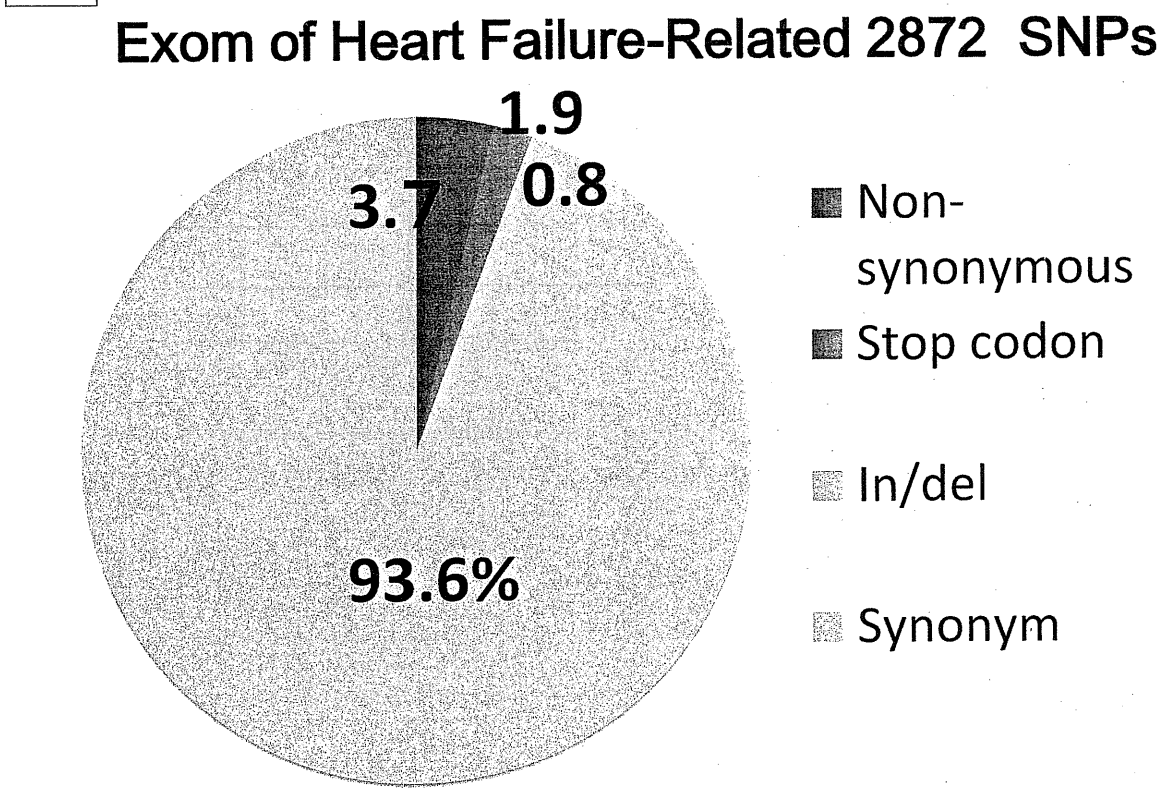

Fig. 3

A

B

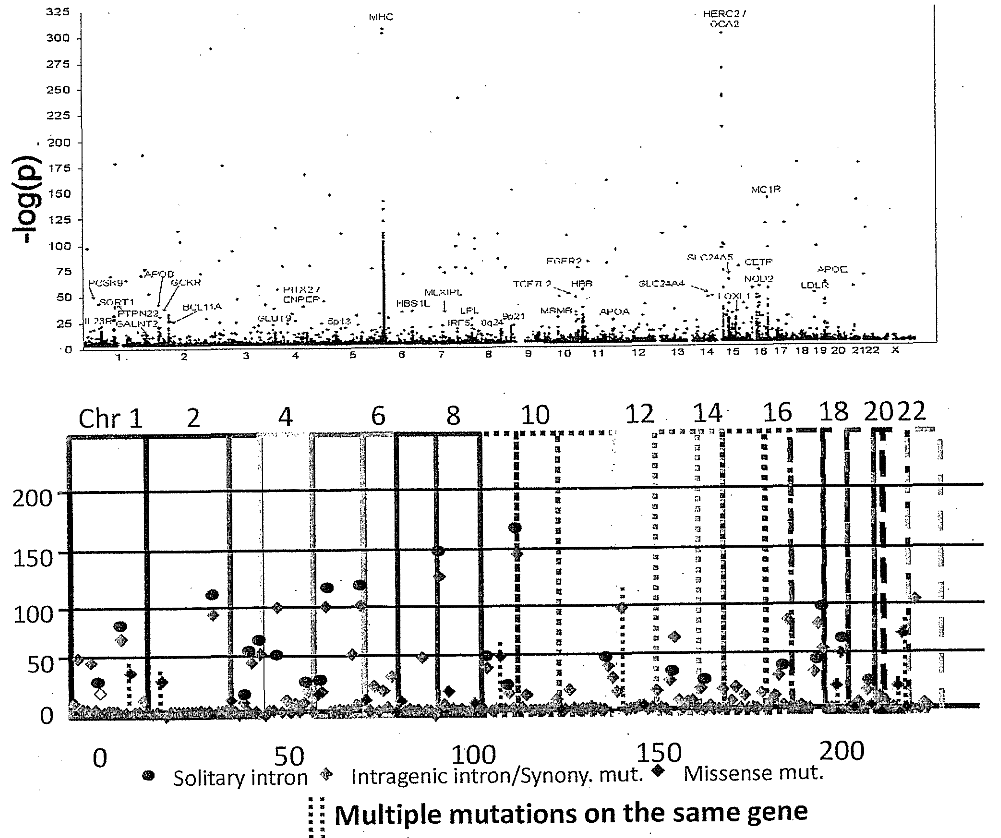

-log(p)
MHC
HERC2 / OCA2
MC1R
Chr 1
Solitary intron
Intragenic intron/Synony. mut.
Missense mut.
Multiple mutations on the same gene

Fig. 4

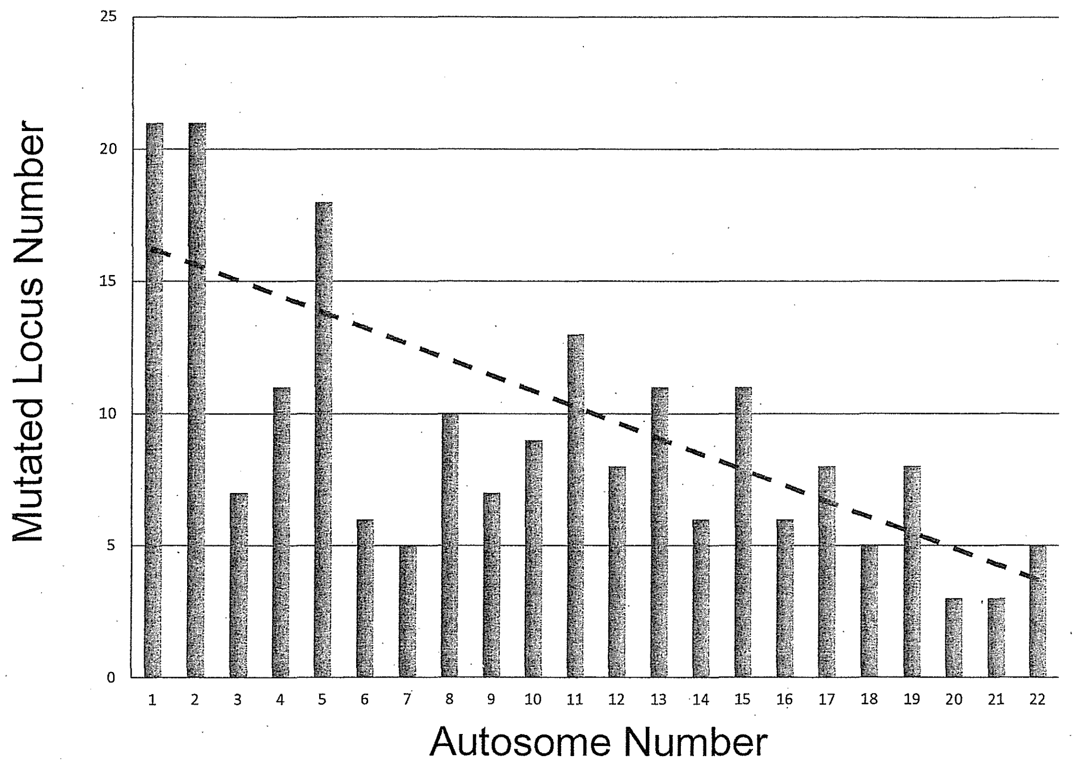

Mutated Locus Number
Autosome Number

Heart Vessels
DOI 10.1007/s00380-012-0252-7

ORIGINAL ARTICLE

Differences in hemodynamic responses between intravenous carperitide and nicorandil in patients with acute heart failure syndromes

Hidetoshi Hattori · Yuichiro Minami · Masayuki Mizuno · Dai Yumino · Hiromi Hoshi · Hiroyuki Arashi · Toshiaki Nuki · Yukiko Sashida · Michiaki Higashitani · Naoki Serizawa · Norihiro Yamada · Junichi Yamaguchi · Fumiaki Mori · Tsuyoshi Shiga · Nobuhisa Hagiwara

Received: 6 February 2012 / Accepted: 23 March 2012

Abstract While recent guidelines for the treatment of acute heart failure syndromes (AHFS) recommend pharmacotherapy with vasodilators in patients without excessively low blood pressure (BP), few reports have compared the relative efficiency of vasodilators on hemodynamics in AHFS patients. The present study aimed to assess the differences in hemodynamic responses between intravenous carperitide and nicorandil in patients with AHFS. Thirty-eight consecutive patients were assigned to receive 48-h continuous infusion of carperitide (n = 19; 0.0125–0.05 μg/kg/min) or nicorandil (n = 19; 0.05–0.2 mg/kg/h). Hemodynamic parameters were estimated at baseline, and 2, 24, and 48 h after drug administration using echocardiography. After 48 h of infusion, systolic BP was significantly more decreased in the carperitide group compared with that in the nicorandil group (22.1 ± 20.0 % vs 5.3 ± 10.4 %, P = 0.003). While both carperitide and nicorandil significantly improved hemodynamic parameters, improvement of estimated pulmonary capillary wedge pressure was greater in the carperitide group (38.2 ± 14.5 % vs 26.5 ± 18.3 %, P = 0.036), and improvement of estimated cardiac output was superior in the nicorandil group (52.1 ± 33.5 % vs 11.4 ± 36.9 %, P = 0.001). Urine output for 48 h was greater in the carperitide group, but not to a statistically significant degree (4203 ± 1542 vs 3627 ± 1074 ml, P = 0.189). Carperitide and nicorandil were differentially effective in improving hemodynamics in AHFS patients. This knowledge may enable physicians in emergency wards to treat and manage patients with AHFS more effectively and safely.

Keywords Acute heart failure · Hemodynamics · Natriuretic peptide · Nicorandil

Introduction

Acute heart failure syndromes (AHFS) are characterized by a gradual or rapid change in the signs and symptoms of heart failure, resulting in the need for urgent treatment [1, 2]. Several recent sets of guidelines for the management of AHFS have suggested that vasodilator therapy should be considered for AHFS patients with a high to normal blood pressure (BP) on admission and should be avoided in those with a low BP [3].

Among the currently available vasodilators, natriuretic peptide preparations such as carperitide and nesiritide (recombinant human atrial and brain natriuretic peptide, respectively) achieve significant reduction of venous and ventricular filling pressures with subsequent rapid improvement of dyspnea or orthopnea [4–6]. Carperitide has been approved for AHFS in Japan, and it was recently reported that signs and symptoms were improved by carperitide therapy in approximately 80 % of AHFS patients with an adequate systolic BP [7, 8].

Nicorandil (*N*-(2-hydroxyethyl)nicotinamide nitrate) has nitrate-like properties, activates adenosine triphosphate-sensitive potassium channels, and results in balanced venous and arterial vasodilation [9, 10]. Nicorandil has also recently been approved for AHFS in Japan, and our prior study suggested that intravenous administration of nicorandil produces optimal benefits in improving hemodynamics in

H. Hattori · Y. Minami (✉) · M. Mizuno · D. Yumino · H. Hoshi · H. Arashi · T. Nuki · Y. Sashida · M. Higashitani · N. Serizawa · N. Yamada · J. Yamaguchi · F. Mori · T. Shiga · N. Hagiwara
Department of Cardiology, Tokyo Women's Medical University, 8-1 Kawada-cho, Shinjuku-ku, Tokyo 162-8666, Japan
e-mail: yuichiro24@celery.ocn.ne.jp

Published online: 19 April 2012

AHFS, as determined by results of noninvasive echocardiographic hemodynamic evaluation [11].

While recent guidelines for the treatment of AHFS recommend pharmacotherapy with vasodilators in patients without excessively low BP, these guidelines do not specifically address the strategy for early medical treatment, because there is limited evidence on the efficacy of the pharmacological agents currently used for AHFS. In addition, few reports have compared the relative efficiency of vasodilators on hemodynamics in AHFS patients. Therefore, the present study aimed to assess the differences in hemodynamic responses between carperitide and nicorandil in patients with AHFS.

Patients and methods

Patients

The study group consisted of 38 consecutive hospitalized patients with AHFS referred to the cardiac intensive care unit at Tokyo Women's Medical University Hospital, who were successfully and accurately assessed for hemodynamic parameters by transthoracic Doppler echocardiography before initial administration of carperitide or nicorandil between May 2008 and August 2010. The diagnosis of heart failure was made based on modified Framingham criteria [12, 13]. In brief, heart failure was diagnosed based on satisfaction of two major criteria or one major and two minor criteria. Acute heart failure syndrome was also defined as the new onset of decompensated heart failure or decompensation of chronic, established heart failure meeting the above criteria and sufficient to warrant hospitalization [1]. We excluded patients who had (1) acute coronary syndrome, (2) moderate to severe valvular heart disease, (3) severe renal insufficiency (serum creatinine >2.0 mg/dl), (4) systolic arterial BP <90 mmHg, (5) pulmonary arterial hypertension with a relevant precapillary component, (6) acutely unstable clinical status not permitting a period of hemodynamic assessment before intravenous vasodilator administration, (7) poor echo window or nonoptimal Doppler signal, or (8) any condition that would contraindicate use of a vasodilator. The study was carried out according to the principles of the Declaration of Helsinki, and the study protocol was approved by the institutional ethics committee. All participating patients gave written informed consent before enrollment.

Protocol

After baseline hemodynamic measurements were recorded, patients were assigned to receive 48 h of continuous infusion of carperitide (0.0125–0.05 μg/kg/min) or nicorandil (0.05–0.2 mg/kg/h) [11, 14]. We used nicorandil between May 2008 and June 2009, and carperitide between July 2009 and August 2010. The doses of carperitide or nicorandil were adjusted according to the condition and systolic BP of each individual patient. Use of intravenous vasodilators or inodilators with the study drug was not permitted. However, prior use of intravenous bolus injection or additional bolus injection of diuretics was permitted. All patients were allowed to continue oral medications used before admission, including diuretics, angiotensin-converting enzyme inhibitors, angiotensin receptor blockers, β-blockers, and digoxin. Hemodynamic measurements were obtained at baseline, and 2, 24, and 48 h after the start of carperitide or nicorandil administration.

Hemodynamic assessment

Hemodynamic evaluation was performed using a cuff sphygmomanometer and transthoracic Doppler echocardiography. Systemic BP was measured noninvasively by a cuff sphygmomanometer. Echocardiographic studies were performed using commercially available ultrasound equipment. A complete M-mode, two-dimensional Doppler study was performed, in the left lateral decubitus or supine position, using standard parasternal, apical, and subcostal approaches. The methods of the noninvasive echocardiographic hemodynamic evaluation have been described previously [11] and are summarized here. Mean right atrial pressure (RAP) was estimated from the inferior vena cava diameter and its degree of respirophasic change [15]. Pulmonary artery systolic pressure (PASP) is equivalent to right ventricular systolic pressure in the absence of obstruction to flow between the right ventricle and pulmonary artery. An estimate of PASP was obtained by adding an estimate of RAP to the systolic transtricuspid pressure gradient [16, 17]. This gradient was estimated by application of the modified Bernoulli equation to the peak velocity of the continuous-wave Doppler tricuspid regurgitation signal. Pulmonary artery end-diastolic pressure is frequently used as an estimate of pulmonary capillary wedge pressure (PCWP). Application of the modified Bernoulli equation to the end-diastolic velocity of the continuous-wave Doppler pulmonary regurgitation signal, and adding to this an estimate of RAP, provided an estimation of PCWP [16, 18]. Estimated cardiac output (CO) was calculated as the product of heart rate, velocity time integral at the left ventricular outflow tract, and the area of the left ventricular outflow tract [19, 20]. Outflow tract diameter was measured with digital calipers in the parasternal long-axis view. All echocardiographic data were obtained by an experienced sonographer and interpreted by two experienced echocardiographers unaware of the patients' participation in the study.

End points

The protocol-specified analyses concerned the hemodynamic effects of carperitide or nicorandil administration in patients with AHFS. The primary end point of the study was the absolute change from baseline in estimated PCWP during carperitide or nicorandil administration. Secondary end points included changes in estimated PASP, estimated CO, and systolic BP. Urine output was measured for 48 h after the start of carperitide or nicorandil administration, and the total dose of intravenous furosemide for 48 h was measured. B-type natriuretic peptide and serum creatinine levels before and after carperitide or nicorandil administration were also measured.

Statistical analysis

Analyses were performed using SAS System version 9.1 software (SAS Institute, Cary, NC, USA). Data are presented as means with standard deviations and frequencies. The Student's *t* test was used to compare groups with respect to normally distributed continuous variables. The Chi-square test or Fisher's exact test (when an expected value was <5) was used to compare nominally scaled variables. For multiple paired time effect comparisons, Dunnett's multiple comparison method was applied. Two-tailed *P* values of less than 0.05 were considered significant.

Results

Baseline characteristics

The baseline demographic, clinical, and hemodynamic characteristics of the 19 patients treated with carperitide and 19 patients treated with nicorandil are shown in Table 1. Before administration of study drugs, no significant differences were observed between the two groups. All patients had dyspnea at rest or New York Heart Association class IV symptoms at the time of infusion, and had clinical evidence of fluid overload.

Table 1 Baseline characteristics of the study patients treated with carperitide or nicorandil

	Carperitide (n = 19)	Nicorandil (n = 19)	P value
Men, n (%)	14 (74)	14 (74)	0.999
Age, years	73 ± 11	69 ± 16	0.398
Ischemic etiology, n (%)	8 (42)	10 (53)	0.516
Medical history, n (%)			
Prior hospitalization for heart failure	9 (47)	12 (63)	0.328
Hypertension	13 (68)	12 (63)	0.732
Diabetes mellitus	7 (37)	8 (42)	0.740
Chronic obstructive pulmonary disease	6 (32)	2 (11)	0.232
Left ventricular ejection fraction, %	34 ± 13	35 ± 15	0.945
Heart rate, beats/min	88 ± 23	76 ± 15	0.073
Blood urea nitrogen, mg/dl	35 ± 17	27 ± 17	0.165
Creatinine, mg/dl	1.4 ± 0.6	1.2 ± 0.5	0.319
Uric acid, mg/dl	7.4 ± 2.3	6.3 ± 1.8	0.181
B-type natriuretic peptide, pg/ml	1083 ± 1131	1741 ± 1265	0.100
Baseline hemodynamic parameters			
Systolic BP, mmHg	141 ± 26	131 ± 31	0.294
Diastolic BP, mmHg	73 ± 15	73 ± 17	0.921
Estimated PASP, mmHg	56 ± 10	51 ± 12	0.217
Estimated PCWP, mmHg	27 ± 5	24 ± 9	0.169
Estimated CO, l/min	3.8 ± 1.3	3.7 ± 1.1	0.845

Values are mean ± SD

BP blood pressure, *CO* cardiac output, *PASP* pulmonary artery systolic pressure, *PCWP* pulmonary capillary wedge pressure

Acute hemodynamic effects of carperitide

After 2 h of carperitide infusion, estimated PCWP was reduced from 27.3 ± 5.0 to 21.0 ± 4.4 mmHg ($P < 0.05$ by Dunnett's multiple comparison method), and was sustained for 48 h to 16.8 ± 4.7 mmHg ($P < 0.05$, Fig. 1a). Estimated PASP was also reduced from 55.5 ± 10.3 to 46.4 ± 8.2 mmHg ($P < 0.05$) after 2 h of carperitide infusion, and was sustained for 48 h to 40.2 ± 12.4 mmHg ($P < 0.05$, Fig. 1b). There was no change in estimated CO over 48 h of carperitide infusion (3.8 ± 1.3 to 4.0 ± 1.8 l/min, *P* not significant; Fig. 1c). Systolic BP was decreased after 2 h of carperitide infusion (140.8 ± 26.3 to 131.4 ± 24.4 mmHg, $P < 0.05$), and was sustained for 48 h (109.1 ± 33.8 mmHg, $P < 0.05$; Fig. 1d). The average dose of intravenous carperitide was 0.022 ± 0.013 μg/kg/min.

Acute hemodynamic effects of nicorandil

After 2 h of nicorandil infusion, estimated PCWP was reduced from 24.0 ± 8.8 to 19.8 ± 7.4 mmHg ($P < 0.05$), and was sustained for 48 h to 17.2 ± 6.3 mmHg ($P < 0.05$, Fig. 1a). Estimated PASP was also reduced from 51.1 ± 11.6 to 43.8 ± 10.9 mmHg ($P < 0.05$) after 2 h of nicorandil infusion, and was sustained for 48 h to 39.4 ± 7.7 mmHg ($P < 0.05$, Fig. 1b). A significant increase in estimated CO was observed at 2 h, from 3.7 ± 1.1 to 4.5 ± 1.3 l/min ($P < 0.05$). This increase in estimated CO was sustained for 48 h to 5.5 ± 1.7 l/min ($P < 0.05$, Fig. 1c). There was a significant decrease in systolic BP after 48 h of